

Lineage switching of the cellular distribution of *BRAF*^{V600E} in multisystem Langerhans cell histiocytosis

Paul Milne,^{1,2} Simon Bomken,^{1,3} Olga Slater,⁴ Ashish Kumar,^{5,6} Adam Nelson,^{5,6} Somak Roy,^{5,7} Jessica Velazquez,⁸ Kshitij Mankad,⁴ James Nicholson,⁹ Dan Yeomanson,¹⁰ Richard Grundy,^{11,12} Ahmed Kamal,¹² Anthony Penn,¹³ Jane Pears,¹⁴ Gerard Millen,¹⁵ Bruce Morland,¹⁵ James Hayden,¹⁶ Jason Lam,^{1,2} Maymoon Madkhali,^{1,17} Jamie MacDonald,^{1,2} Preeti Singh,^{1,2} Sarah Pagan,^{1,2} Carlos Rodriguez-Galindo,¹⁸ Milen Minkov,¹⁹ Jean Donadieu,²⁰ Jennifer Picarsic,^{5,7} Carl Allen,⁸ Venetia Bigley,^{1,2} and Matthew Collin^{1,2}

¹Translational and Clinical Research Institute, Newcastle University, Newcastle upon Tyne, United Kingdom; ²National Institute for Health and Care Research, Newcastle Biomedical Research Centre, Newcastle upon Tyne, United Kingdom; ³Newcastle upon Tyne Hospitals NHS Foundation Trust, Newcastle upon Tyne, United Kingdom; ⁴Great Ormond Street Hospital for Children NHS Foundation Trust, London, United Kingdom; ⁵Department of Pediatrics, University of Cincinnati College of Medicine, Cincinnati, OH; ⁶Division of Bone Marrow Transplantation and Immune Deficiency and ⁷Division of Pathology and Laboratory Medicine, Cincinnati Children's Hospital Medical Center, Cincinnati, OH; ⁸Texas Children's Cancer and Hematology Centers, Texas Children's Hospital, Baylor College of Medicine, Houston, TX; ⁹Addenbrooke's Hospital, Cambridge University Hospitals NHS Foundation Trust, Cambridge, United Kingdom; ¹⁰Sheffield Children's Hospital, Sheffield Children's NHS Foundation Trust, Sheffield, United Kingdom; ¹¹Children's Brain Tumour Research Centre, University of Nottingham, Nottingham, United Kingdom; ¹²Nottingham Children's Hospital, Queen's Medical Centre, Nottingham University Hospitals NHS Trust, Nottingham, United Kingdom; ¹³Royal Manchester Children's Hospital, Manchester University, NHS Foundation Trust, Manchester, United Kingdom; ¹⁴Children's Health Ireland, Dublin, Ireland; ¹⁵Haematology and Oncology, Birmingham Women's and Children's NHS Foundation Trust, Birmingham, United Kingdom; ¹⁶Paediatric Oncology, Alder Hey Children's NHS Foundation Trust, Liverpool, United Kingdom; ¹⁷Department of Laboratory and Blood Bank, Samtah General Hospital, Jazan Health, Ministry of Health, Samtah, Kingdom of Saudi Arabia; ¹⁸St. Jude Children's Research Hospital, Memphis, TN; ¹⁹St. Anna Children's Hospital, Children's Cancer Research Institute, Vienna, Austria; and ²⁰Department of Pediatric Haematology and Oncology, Hôpital Armand-Trousseau, Assistance Publique-Hôpitaux de Paris (AP-HP), Paris, France

Key Points

- *BRAF*^{V600E} alleles are mainly found in myeloid cells at diagnosis of multisystem LCH.
- After more than 2 years, T cells account for 85% of persistent *BRAF*^{V600E} mutation detected in peripheral blood mononuclear cells.

Most children with high-risk Langerhans cell histiocytosis (LCH) have *BRAF*^{V600E} mutation. *BRAF*^{V600E} alleles are detectable in myeloid mononuclear cells at diagnosis but it is not known if the cellular distribution of mutation evolves over time. Here, the profiles of 16 patients with high-risk disease were analyzed. Two received conventional salvage chemotherapy, 4 patients on inhibitors were tracked at intervals of 3 to 6 years, and 10 patients, also given inhibitors, were analyzed more than 2 years after diagnosis. In contrast to the patients responding to salvage chemotherapy who completely cleared *BRAF*^{V600E} within 6 months, children who received inhibitors maintained high *BRAF*^{V600E} alleles in their blood. At diagnosis, mutation was detected predominantly in monocytes and myeloid dendritic cells. With time, mutation switched to the T-cell compartment, which accounted for most of the mutational burden in peripheral blood mononuclear cells, more than 2 years from diagnosis (median, 85.4%; range, 44.5%-100%). The highest level of mutation occurred in naïve CD4⁺ T cells (median, 51.2%; range, 3.8%-93.5%). This study reveals an unexpected lineage switch of *BRAF*^{V600E} mutation in high-risk LCH, which may influence monitoring strategies for the potential withdrawal of inhibitor treatment and has new implications for the pathogenesis of neurodegeneration, which occurred in 4 patients.

Submitted 30 November 2021; accepted 13 August 2022; prepublished online on *Blood Advances* First Edition 16 September 2022; final version published online 15 May 2023. <https://doi.org/10.1182/bloodadvances.2021006732>.

Data are available on request from the corresponding author, Matthew Collin (matthew.collin@newcastle.ac.uk).

The full-text version of this article contains a data supplement.

© 2023 by The American Society of Hematology. Licensed under [Creative Commons Attribution-NonCommercial-NoDerivatives 4.0 International \(CC BY-NC-ND 4.0\)](https://creativecommons.org/licenses/by-nc-nd/4.0/), permitting only noncommercial, nonderivative use with attribution. All other rights reserved.

Introduction

Langerhans cell histiocytosis (LCH) is a histiocytic neoplasm associated with inappropriate *MAPK* activation, caused by somatic mutation or fusion of *BRAF* or other *MAPK* pathway genes.¹⁻³ LCH cells accumulate, forming destructive lesions and impairing organ function. Multisystem LCH (MS-LCH) with risk organ involvement affects the bone marrow, liver, and spleen leading to death in up to 10% of cases.⁴ When *BRAF*^{V600E} is present in patients with high-risk disease, mutation is detectable in cellular DNA isolated from monocytes and myeloid dendritic cells (DCs).⁵⁻¹⁰

BRAF and *MEK* inhibitors can induce dramatic clinical improvement in patients with MS-LCH with risk organ involvement who fail salvage chemotherapy.¹¹⁻¹⁶ However, many studies have shown that 1% to 10% of *BRAF*^{V600E} alleles persist in peripheral blood mononuclear cells (PBMCs) and cell-free DNA, and that treatment withdrawal often results in rapid relapse.¹¹⁻¹⁶ Because monocytes and myeloid DCs are potential precursors of LCH cells, this has led to the assumption that mutation persists mainly in the myeloid cell compartment. In this study, we performed longitudinal and cross-sectional analyses of patients with high-risk LCH from 3 centers and found that the persistence of mutation in peripheral blood was associated with switching of the reservoir from myeloid cells to T cells.

Methods

Patients and samples

Samples were obtained from UK patients joining the LCHIV Biology Study sponsored by Newcastle upon Tyne Hospitals NHS Foundation Trust (Newcastle upon Tyne, United Kingdom) with informed consent according to research ethics committee-approved study protocols. Blood samples from Cincinnati, Ohio, and Houston, Texas, were collected from patients with LCH under protocols approved by the institutional review boards of Cincinnati Children's Hospital Medical Center and Baylor College of Medicine, respectively.

Full clinical details are given in the supplemental material and supplemental Table 1.

Flow cytometry

Absolute quantitation was performed using TruCount tubes (Becton Dickinson Biosciences), acquired on an LSRFortessa X-20 (Becton Dickinson Biosciences), and analyzed with FlowJo version 10.7.1 (Tree Star). Mononuclear cells were sorted using a BD FACSAria Fusion System (Becton Dickinson Biosciences). Antibodies and gating are given in supplemental Table 2 and supplemental Figure 1.

Measurement of *BRAF*^{V600E}

DNA was extracted using QIAamp Micro/Mini and Circulating Nucleated Acid Kits (Qiagen). *BRAF* mutation was measured with mutation allele assay, *BRAF*_476_mu 4465804 Hs00000111_mu and gene reference assay, *BRAF*_rf 4465807 Hs00000172_rf (Life Technologies) on QuantStudio 3 Real-Time PCR System (ThermoFisher Scientific) with 50 cycles. $C_{t_{mutant}}$ and $C_{t_{reference\ wild-type}}$ values were manually inspected and compared with negative controls as described in the supplemental information and supplemental Figure 2. The fraction of mutated alleles was calculated from

$1/2^{[C_{t_{reference\ wild-type}} - C_{t_{mutant}}]}$. The fraction of mutated cells is double this value, assuming heterozygous mutation. The absolute number of mutated cells per μL is the product of the absolute cell count and the fraction of mutated cells. The percentage contribution to mutation burden is the proportion contributed by each cell type of the sum of all of the mutated alleles measured. Graphs and statistics were done with Prism version 5.0 (GraphPad Software Inc).

Results and discussion

The kinetics of *BRAF*^{V600E} mutation were observed in 2 patients undergoing salvage chemotherapy with cladribine and cytarabine. The level of *BRAF*^{V600E} declined in parallel with clinical improvement, until it was undetectable (Figure 1A). During treatment, mutation was slightly higher in plasma cell-free DNA than in PBMC (supplemental Figure 3A). Although these patients remained in clinical remission with undetectable mutation more than 3 years later, 4 patients who failed salvage chemotherapy and were treated with *MAPK* inhibitors rapidly improved but maintained a high level of mutant alleles at similar levels in PBMC and plasma cell-free DNA (Figure 1B; supplemental Figure 3B).

As previously reported, mutation was mainly present in CD14⁺ classical monocytes, CD16⁺ nonclassical monocytes, and CD1c⁺ myeloid DCs at diagnosis.⁵⁻¹⁰ Lymphoid cells including CD3⁺ T cells, CD19⁺ B cells, and CD56⁺ natural killer cells were either an order of magnitude lower or negative at this point. However, with time, we observed an increase in both the mutated allele fraction and the absolute number of mutated alleles per μL , attributable to T cells. At 1.5 to 4.5 years after diagnosis, the mutation burden of T cells exceeded that of myeloid cells (Figure 1B).

Early attempts to withdraw inhibitor therapy were not successful in patient 3. However, patients 4 and 6 were successfully moved to oral maintenance with 6-mercaptopurine and methotrexate, without systemic relapse at the point at which *BRAF*^{V600E} had switched completely to T cells (Figure 1B). Patient 6 had also received high-dose chemotherapy during treatment with trametinib, a strategy also reported by others in association with clearance of mutation.¹⁸ However, in our patients, *BRAF*^{V600E} persisted in T cells, but systemic disease did not recur. Further studies will be required to determine whether these observations are causally related.

Seeking to validate the observation that mutation switched from myeloid cells to T cells and to exclude the contribution of other lymphoid cells that had not been directly measured in the first cohort, we recruited a second cohort of 10 patients. A single blood sample was obtained at least 2 years after diagnosis and between 6 months and 5 years on inhibitor therapy. This confirmed that a median of 85.4% of mutated alleles were present in T cells, compared with 2.7% in B cells, 2.8% in natural killer cells, and 0.3% in myeloid cells (Figure 2A). Granulocytes were consistently negative in our hands at all time points.⁷ *BRAF*^{V600E} was most abundant in naïve CD4⁺ and CD8⁺ cells, suggesting that enrichment in the T-cell lineage was not simply because of the expansion of memory clones (Figure 2B). Combining the data from all patients in both cohorts, we observed that the level of mutation remained roughly constant in PBMC, but with time, switched from myeloid to T cells (Figure 2C-D).

Most reports agree that *BRAF*^{V600E} is found primarily in myeloid cells at diagnosis of MS-LCH.^{5-10,13} Mutation has previously been reported exclusively in T cells of 1 patient treated with inhibitors

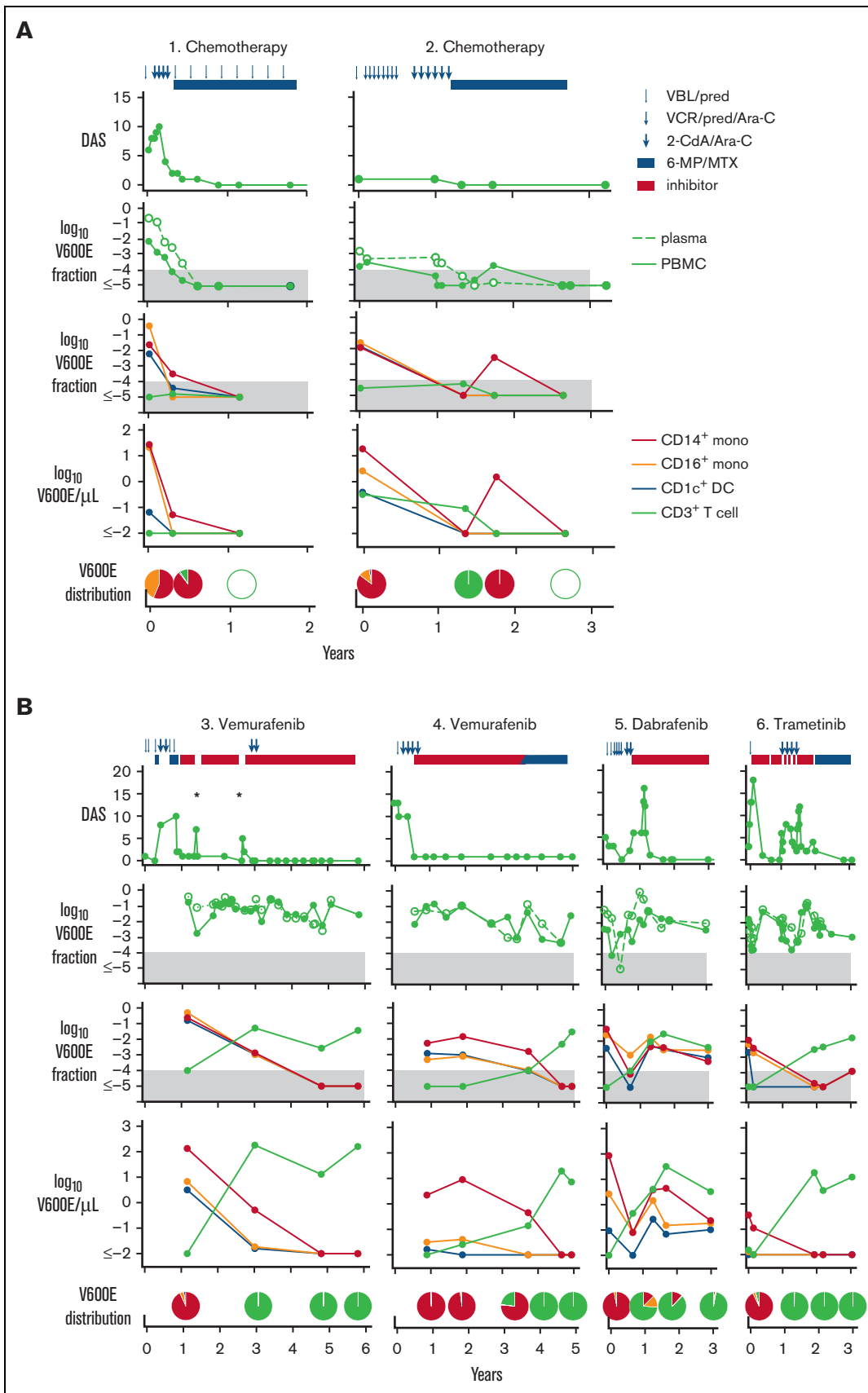


Figure 1.

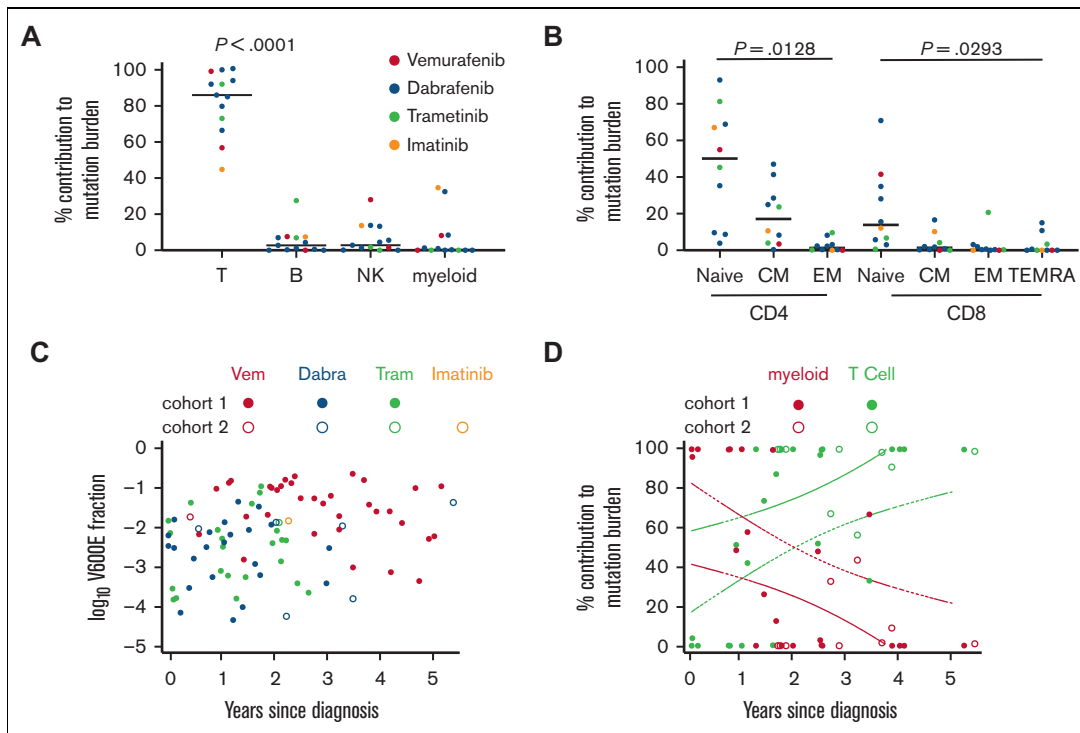


Figure 2. Comparison and quantitation of alleles in lymphoid subsets. (A) The percentage contribution of each PBMC subset to the total mutation burden (obtained by summing the parts) among CD3⁺ T cells, CD19⁺ B cells, and myeloid cells (monocytes and DCs). (B) The percentage contribution of each T-cell subset to the mutation burden present in T cells among naïve, central memory (CM), effector memory (EM), and effector memory cells re-expressing CD45RA (TEMRA). Supplemental Figure 1 shows the sorting strategy. In panels A and B, the graphs show data from 1 late time point of all patients with a sufficient material available (n = 13; analysis of variance). (C) Summary of the mutant allele fraction in PBMC in all samples as a function of time on treatment. (D) Summary of the percentage contribution from T cells (green) and all myeloid cells (red) to the total mutation burden of these subsets as a function of time since diagnosis (n = 33). Broken lines depict the 95% confidence intervals for a simple linear regression. Dabra, dabrafenib; NK, natural killer; Tram, trametinib; Vem, vemurafenib.

who had undergone stem cell transplantation.¹³ Our data now show that T cells become the dominant reservoir in all patients with high-risk LCH with persisting mutation. Although most of the patients in this study had been maintained on MAPK inhibitor therapy for several years, 1 received imatinib and 2 were diagnosed more than 4 years earlier, before being switched to MAPK inhibitors for only 6 to 12 months before sampling. Although it is conceivable that MAPK inhibitors might exert a greater selective pressure on myeloid-primed progenitors allowing lymphoid lineages to grow out, inhibitor treatment may have simply allowed us to observe a natural time-dependent process in patients with high-risk disease.

Although we noted that 2 patients who received chemotherapy with MAPK inhibitors were able to withdraw from inhibitors, the

confinement of mutation to T cells may not correlate with safe treatment cessation in all patients. Vigilance for late effects must also be maintained. Patient 4 developed neurodegeneration 1 year after vemurafenib was withdrawn (supplemental Figure 5), and 3 patients in cohort 2 developed neurodegeneration just before starting inhibitor therapy. In all, their T cells accounted for >90% of *BRAF*^{V600E}, at the onset of symptoms. Mutation has previously been reported in the T cells of conventionally treated patients who developed neurodegeneration¹⁹ and are known to access the central nervous system in other forms of neuropathology.²⁰ Given the similar latency of lineage switching and the onset of neurodegeneration, it will be of great interest to determine whether there is a causal link with T cells carrying activated *BRAF*.

Figure 1. Clinical progress and distribution of *BRAF*^{V600E} alleles in PBMC and sorted cell fractions. (A) Patients 1 and 2 treated with conventional chemotherapy. (B) Patients 3 to 6 treated with inhibitors. Pie charts depict the distribution of mutated cells as a proportion of all mutated cells detected in blood. Each chart is aligned as closely as possible to the corresponding time point. Blue symbols at the top indicate chemotherapy cycles; red bar indicates MAPK inhibitor. Clinical scores and mutation analyses over time are shown in rows (top to bottom). Filled gray areas indicate negative results below 0.0001. Disease Activity Score (DAS) was measured according to Donadieu et al¹⁷; *BRAF*^{V600E} mutation fraction measured in total PBMC (filled symbols and lines) and plasma cell-free DNA (open symbols and broken line); *BRAF*^{V600E} mutation fraction measured in sorted subsets; and mutated cells per μ L in sorted subsets. Asterisks indicate rapid disease reactivation when treatment was suspended. Red line indicates classical CD14⁺ monocytes; orange line indicates CD16⁺ nonclassical monocytes; blue line indicates CD1c⁺ myeloid DC; and green line indicates CD3⁺ T cells. VBL/pred, vinblastine and prednisone; VCR/pred/Ara-C, vincristine, prednisone, and cytarabine; 2CdA/Ara-C, cladribine and cytarabine; 6-MP/MTX: 6-mercaptopurine and methotrexate maintenance.

Acknowledgments

The authors thank the patients and families who participated in this study.

This work was supported by funding from the Cancer Research UK biomarker project (grant C30484/A21025), Histo UK, Histiocytosis Association, and Bright Red.

This work would not have been possible without the inspiration and enthusiasm of our late friend and colleague, Johann Visser.

Authorship

Contribution: P.M. designed and performed experiments, interpreted data, and wrote the manuscript; S.B., A. Kumar, and C.A. provided samples and clinical data and interpreted data; O.S., J.N., D.Y., R.G., A.P., J. Pears, G.M., B.M., and J.H. provided samples and clinical data; A.N., S.R., and J.V. provided samples; K.M. provided and interpreted clinical data; A. Kamal, C.R.-G., and M. Minkov provided clinical data; J.L., M. Madhkali, J.M., and P.S. processed samples; S.P. coordinated sample collection and

processing; J.D. and V.B. interpreted data; J. Picarsic provided samples and interpreted data; and M.C. designed experiments, interpreted data, and wrote the manuscript.

Conflict-of-interest disclosure: A. Kumar is a consultant for Sobi and SpringWorks Therapeutics. The remaining authors declare no competing financial interests.

ORCID profiles: P.M., [0000-0002-8278-0463](https://orcid.org/0000-0002-8278-0463); S.B., [0001-9163-5738](https://orcid.org/0001-9163-5738); A.K., [0000-0002-8306-8419](https://orcid.org/0000-0002-8306-8419); S.R., [0000-0002-5681-0112](https://orcid.org/0000-0002-5681-0112); K.M., [0000-0001-5979-9337](https://orcid.org/0000-0001-5979-9337); J.N., [0000-0001-9494-0199](https://orcid.org/0000-0001-9494-0199); R.G., [0000-0002-2585-2539](https://orcid.org/0000-0002-2585-2539); G.M., [0000-0003-1446-3228](https://orcid.org/0000-0003-1446-3228); M. Madhkali, [0000-0002-9424-0966](https://orcid.org/0000-0002-9424-0966); C.R.-G., [0000-0002-2360-8946](https://orcid.org/0000-0002-2360-8946); M. Minkov, [0000-0001-6471-8423](https://orcid.org/0000-0001-6471-8423); J.D., [0000-0002-4485-146X](https://orcid.org/0000-0002-4485-146X); J. Picarsic, [0000-0002-3718-6422](https://orcid.org/0000-0002-3718-6422); M.C., [0000-0001-6585-9586](https://orcid.org/0000-0001-6585-9586).

Correspondence: Matthew Collin, Translational and Clinical Research Institute, Newcastle University, Framlington Place, Newcastle upon Tyne NE2 4HH, United Kingdom; email: matthew.collin@newcastle.ac.uk.

References

1. Allen CE, Beverley PCL, Collin M, et al. The coming of age of Langerhans cell histiocytosis. *Nat Immunol*. 2020;21(1):1-7.
2. Chakraborty R, Abdel-Wahab O, Durham BH. MAP-kinase-driven hematopoietic neoplasms: a decade of progress in the molecular age. *Cold Spring Harb Perspect Med*. 2020;11(5):a034892.
3. McClain KL, Bigenwald C, Collin M, et al. Histiocytic disorders. *Nat Rev Dis Prim*. 2021;7(1):73.
4. Gardner H, Minkov M, Grois N, et al. Therapy prolongation improves outcome in multisystem Langerhans cell histiocytosis. *Blood*. 2013;121(25):5006-5014.
5. Berres ML, Lim KP, Peters T, et al. BRAF-V600E expression in precursor versus differentiated dendritic cells defines clinically distinct LCH risk groups. *J Exp Med*. 2014;211(4):669-683.
6. Héritier S, Hélias-Rodzewicz Z, Lapillonne H, et al. Circulating cell-free BRAF(V600E) as a biomarker in children with Langerhans cell histiocytosis. *Br J Haematol*. 2017;178(3):457-467.
7. Milne P, Bigley V, Bacon CM, et al. Hematopoietic origin of Langerhans cell histiocytosis and Erdheim-Chester disease in adults. *Blood*. 2017;130(2):167-175.
8. Durham BH, Roos-Weil D, Baillou C, et al. Functional evidence for derivation of systemic histiocytic neoplasms from hematopoietic stem/progenitor cells. *Blood*. 2017;130(2):176-180.
9. Lim KPH, Milne P, Poidinger M, et al. Circulating CD1c⁺ myeloid dendritic cells are potential precursors to LCH lesion CD1a⁺CD207⁺ cells. *Blood Adv*. 2020;4(1):87-99.
10. Xiao Y, van Halteren AGS, Lei X, et al. Bone marrow-derived myeloid progenitors as driver mutation carriers in high- and low-risk Langerhans cell histiocytosis. *Blood*. 2020;136(19):2188-2199.
11. Donadieu J, Larabi IA, Tardieu M, et al. Vemurafenib for refractory multisystem Langerhans cell histiocytosis in children: an international observational study. *J Clin Oncol*. 2019;37(31):2857-2865.
12. Eckstein OS, Visser J, Rodriguez-Galindo C, Allen CE; NACHO-LIBRE Study Group. Clinical responses and persistent BRAF V600E⁺ blood cells in children with LCH treated with MAPK pathway inhibition. [letter]. *Blood*. 2019;133(15):1691-1694.
13. Schwentner R, Kolenová A, Jug G, et al. Longitudinal assessment of peripheral blood BRAFV600E levels in patients with Langerhans cell histiocytosis. *Pediatr Res*. 2019;85(6):856-864.
14. Hazim AZ, Ruan GJ, Ravindran A, et al. Efficacy of BRAF-inhibitor therapy in BRAF^{V600E}-mutated adult Langerhans cell histiocytosis. *Oncologist*. 2020;25(12):1001-1004.
15. Evseev D, Kalinina I, Raykina E, et al. Vemurafenib provides a rapid and robust clinical response in pediatric Langerhans cell histiocytosis with the BRAF V600E mutation but does not eliminate low-level minimal residual disease per ddPCR using cell-free circulating DNA. *Int J Hematol*. 2021;114(6):725-734.

16. Yang Y, Wang D, Cui L, et al. Effectiveness and safety of dabrafenib in the treatment of 20 Chinese children with BRAFV600E-mutated Langerhans cell histiocytosis. *Cancer Res Treat.* 2021;53(1):261-269.
17. Donadieu J, Piguet C, Bernard F, et al. A new clinical score for disease activity in Langerhans cell histiocytosis. *Pediatr Blood Cancer.* 2004;43(7):770-776.
18. Eder SK, Schwentner R, Ben Soussia P, et al. Vemurafenib acts as molecular on-off switch governing systemic inflammation in Langerhans cell histiocytosis. *Blood Adv.* 2021;6(3):970-975.
19. McClain KL, Picarsic J, Chakraborty R, et al. CNS Langerhans cell histiocytosis: common hematopoietic origin for LCH-associated neurodegeneration and mass lesions. *Cancer.* 2018;124(12):2607-2620.
20. Smolders J, van Luijn MM, Hsiao CC, Hamann J. T-cell surveillance of the human brain in health and multiple sclerosis. *Semin Immunopathol.* 2022;44(6):855-867.